

Method for correcting remanent fields in magnetic property measurement systems without field compensation.

Simo Spassov⁽¹⁾ & Ramon Egli⁽²⁾

⁽¹⁾Geophysical Centre of the Royal Meteorological Institute of Belgium, 1 rue du Centre Physique, B-5670 Dourbes (Viroinval) Belgium.

⁽²⁾Zentralanstalt für Meteorologie und Geodynamik, Hohe Warte 38, 1190 Wien, Austria.

simo@meteo.be

08. XII. 2016

1. Introduction

Certain types of magnetic property measurement systems sense the applied magnetic field indirectly through the net current applied to the superconducting magnet solenoid [1]. Even if the current value is converted to a field through an appropriated calibration coefficient, the actual field at the sample location might still differ from the nominal value [2]. In case of superconducting magnets, differences between nominal and true applied field can originate from small persistent currents associated with magnetic flux trapping. These currents generate an additional remanent magnetic field, whose amplitude depends on the field sweeping history of the magnet [1]. Particularly when measuring in the low-field region, this field can cause measurement artefacts, such as inverted hysteresis branches yielding a negative apparent coercivity [2] (Fig. 1), or ZFC warming curves starting with a negative offset. The remanent field can be reduced or eliminated by magnet quenching, zeroing in oscillating mode, or by applying an opposite field [3]. Unfortunately, neither method is suitable for hysteresis measurements, where the field is monotonically swept between two extreme values.

A suitable post-measurement correction method for hysteresis measurements is proposed in the following.

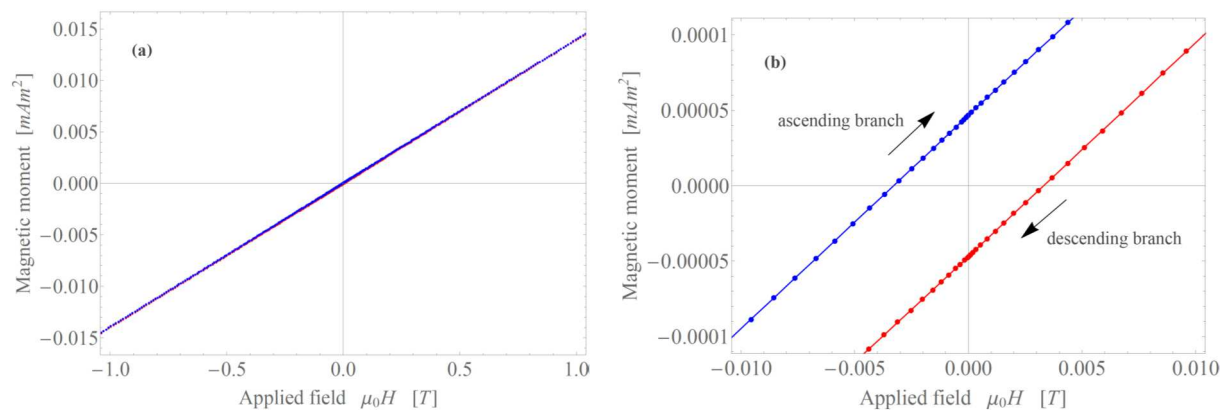


Figure 1: Hysteresis measurement of the paramagnetic *Pd* standard sample between ± 7 T. **a)** Plot over ± 1 T showing a linear $M(H)$ curve crossing apparently at $M(0) = 0$. Both hysteresis branches seem to overlap, as expected for paramagnetic materials. **b)** Detail of the same hysteresis loop over ± 0.01 T. The descending branch

(red) crosses the field axis at about $+3.5 \text{ mT}$ and the ascending branch (blue) at -3.5 mT , pointing to a negative coercivity $H_c = -3.5 \text{ mT}$.

2. Measurement procedure

High-resolution four-quadrant magnetic hysteresis measurements were performed on a MPMS3 system using a paramagnetic Palladium calibration sample. Following measurement parameters were used:

- VSM mode
 - Peak vibration amplitude: 2 mm
 - Averaging time: 5 s
- Field setting
 - Stable at each field
 - Sweep rate 10 mT/s
- Data acquisition
 - 500 points per hysteresis branch
 - Uniform spacing in \sqrt{H} steps

Several hysteresis loops $M(H)$ have been measured over the following field ranges: $\pm 0.5 \text{ T}$, $\pm 1 \text{ T}$, $\pm 2 \text{ T}$, $\pm 3 \text{ T}$, $\pm 5 \text{ T}$ and $\pm 7 \text{ T}$. All measurements started at the maximum field in the 1st quadrant, e.g. $+7 \text{ T} \rightarrow 0 \text{ T} \rightarrow -7 \text{ T} \rightarrow 0 \text{ T} \rightarrow +7 \text{ T}$.

Preliminary experiments were carried out at lower field resolution and at temperatures of 100 K and 300 K to check for a possible temperature dependence of the field error. Such temperature dependence is expected only in case of a sample-related origin of the apparent negative coercivities, since the measurement chamber is thermally insulated from the superconducting magnet. These preliminary experiments confirmed the temperature independence of the remanent field error. All high-resolution experiments discussed in the following were carried out at 300 K .

3. Data correction procedure

The field correction procedure is based on the assumption that the open loop of the paramagnetic Pd sample is caused by an additional “frozen-flux” field $H_{\text{ff}}(H, H_{\text{max}})$, which depends on the maximum applied field H_{max} of the hysteresis measurement (e.g. 7 T in case of $\pm 7 \text{ T}$ hysteresis), and the nominal applied field H . The measured hysteresis loop is then given by

$$M^\pm(H) = M_i^\pm(H + H_{\text{ff}}^\pm), \quad (1)$$

where M_i is the intrinsic, artefact-free hysteresis loop, with “+” and “-” denoting the descending and the ascending branch, respectively. In case of a paramagnetic sample with $M_i^+ = M_i^- = \chi_p H$, eq. (1) can be solved with respect to H_{ff}^\pm , obtaining

$$H_{\text{ff}}^\pm(H) = \frac{M^\pm(H)}{\chi_p} - H. \quad (2)$$

The paramagnetic susceptibility χ_p is not known a-priori, but can be determined by solving eq. (2) for the special case $H = -H_{\text{max}}$, where the two measured branches coincide, so that $H_{\text{ff}}^\pm(-H_{\text{max}}) = 0$ and

$$\chi_p = H_{\text{ff}}^\pm(H) = \frac{-M^\pm(-H_{\text{max}})}{H_{\text{max}}} \quad (3)$$

An example of frozen flux field calculated with eq. (2-3) from measurements of the Pd sample up to 7 T is shown in Fig. 2. When starting from $\pm H_{\text{max}}$, H_{ff} is characterized by an initial, exponential-like approach to a plateau value of $\pm 1 \text{ mT}$, which is particularly pronounced along the descending branch,

and is responsible for the small closure error of the loop, that is the difference between the first measurement $M^+(H_{\max})$ and the last measurement $M^-(H_{\max})$. The strongest variations of H_{ff} occur around $H = 0$, with a relatively sharp increase to ± 4 mT, followed by a progressive decay until the end of the measured branch is reached. H_{ff}^+ and H_{ff}^- are related to each other by the same type of symmetry as the major hysteresis loop, that is $H_{\text{ff}}^-(H) = -H_{\text{ff}}^+(-H)$, up to the abovementioned closure error in proximity of $+H_{\max}$.

The starting point for the field correction is the calculation field difference between descending and ascending hysteresis branch ΔH . The inverses of both branches, *i.e.* $H(M)$, were interpolated and the field difference between both calculated. Figure 2 reveals that this difference is linear by no means. It peaks in the zero field region and wanes towards the strong field regions. Having a closer look, one recognises that the curve is somewhat asymmetric. It does not show an asymptotic behaviour in the strong field regions. Apart from two extreme values in the positive field range at around 0 and 2 T, noise increases towards the strong-field region.

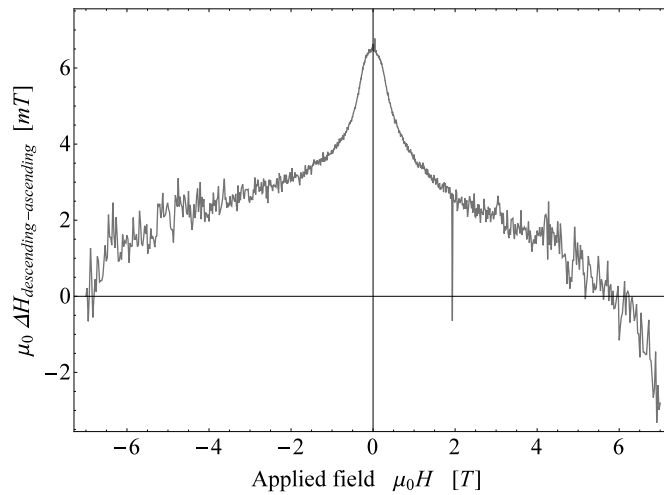


Figure 2: Calculated field difference between descending and ascending branch in dependence of the applied field, *i.e.* $\Delta H(H)$ for the Pd standard sample measured between ± 7 T.

For applying a correction, the difference curve has to be fitted with an appropriate function. Due to the aforementioned asymmetry two separate functions were used for positive and negative fields:

- Positive applied fields: $f_P(H) = a \text{Tanh} \left[\frac{1}{bH} \right] + \sum_{i=0}^5 c_i c H^i \quad \forall H > 0 \quad (1)$
- Negative applied fields: $f_N(H) = -a \text{Tanh} \left[\frac{1}{bH} \right] + \sum_{i=0}^5 c_i c H^i \quad \forall H < 0 \quad (2)$

H being the applied field, *i.e.* in the present case the reported value for the descending branch.

Fitting was done in two steps. An initial fit was solely performed for calculating the fit residuals serving as weights for the final fit. Given the increasing noise in the strong-field regions the initial fit was weighted by $1/\sqrt{H}$. Weighing was necessary to suppress the influence of extreme values, *e.g.* Fig. 2 at $+2$ T.

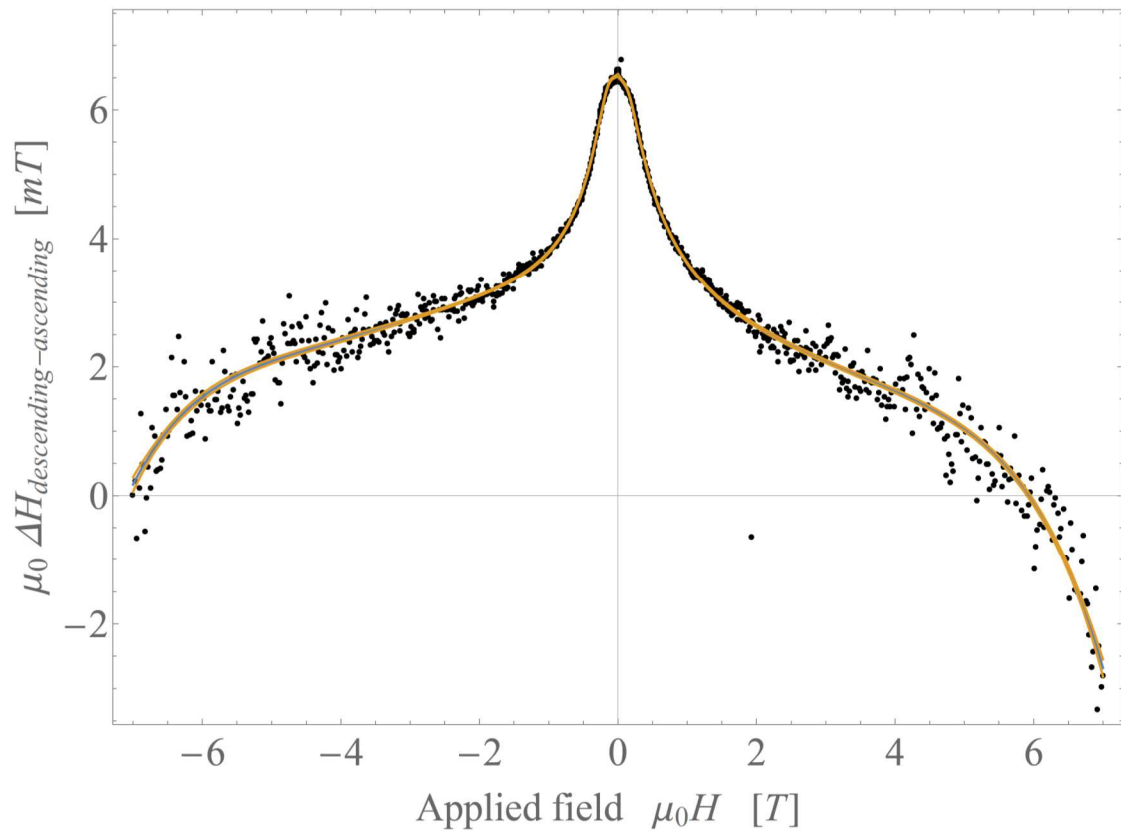


Figure 3: Calculated differences between descending and ascending branch (black dots) $\Delta H(H)$ and best fits for positive and negative field range according to equations (1) and (2). The two yellow lines around the best fit (blue) represent the error envelope of the mean best fit at a confidence level of 99 %. For further details see text.

For the difference curve in Figure 2, following parameter vectors were obtained for both best fits, cf. Figure 3:

Positive applied fields

$$\{a \rightarrow 2.835, b \rightarrow 0.336, c_0 \rightarrow 3.702, c_1 \rightarrow -1.416, c_2 \rightarrow 0.550, c_3 \rightarrow -0.156, c_4 \rightarrow 0.025, c_5 \rightarrow 0.002\}$$

$$\bar{R}^2 = 0.999871$$

Negative applied fields:

$$\{a \rightarrow -3.458, b \rightarrow 0.315, c_0 \rightarrow 3.080, c_1 \rightarrow 0.595, c_2 \rightarrow 0.369, c_3 \rightarrow 0.142, c_4 \rightarrow 0.025, c_5 \rightarrow 0.002\}$$

$$\bar{R}^2 = 0.999878$$

\bar{R}^2 is the coefficient of determination R^2 , adjusted for the number of fit parameters,

$$\bar{R}^2 = 1 - \frac{n-1}{n-p}(1 - R^2) \quad (3)$$

with n being the number of measured data per branch and p the number of fit parameters.

Next, the measured $M(H)$ curves of each quadrant were corrected by subtracting or adding the corresponding fitted functions:

Descending branch

1st Quadrant [+7 ; 0T]

$$\bullet \quad M(H_{corr}) = M(H - \frac{1}{2}f_P(H)) \quad (3)$$

2nd Quadrant [0 ; -7T]

$$\bullet \quad M(H_{corr}) = M(H - \frac{1}{2}f_N(H)) \quad (4)$$

Ascending branch

3rd Quadrant [-7 ; 0T]

$$\bullet \quad M(H_{corr}) = M(H + \frac{1}{2}f_N(H)) \quad (5)$$

4th Quadrant [0 ; +7T]

$$\bullet \quad M(H_{corr}) = M(H + \frac{1}{2}f_P(H)) \quad (6)$$

The result of this correction is given Fig. 4 demonstrating that both hysteresis branches almost coincide in the zero field region.

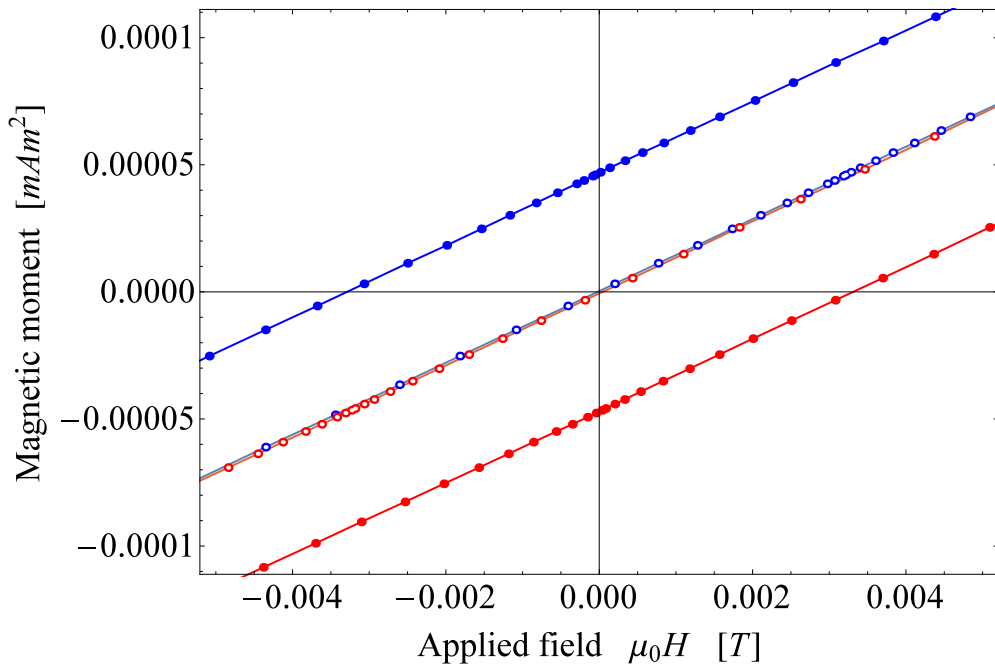


Figure 4: Corrected $M(H)$ curve of the paramagnetic Pd standard sample (open circles). For comparison the uncorrected curve is also given (filled circles). Red and blue colour refer to the descending and the ascending $M(H)$ branches, respectively.

In order to check if the correction was properly done over the whole field range measured, $\Delta H(H)$ for the corrected $M(H)_{corr}$ loop was calculated. It is well demonstrated in Fig. 5 that ΔH oscillates around zero after the correction, and that no systematic trend is seen. In contrast, the random error is persisting.

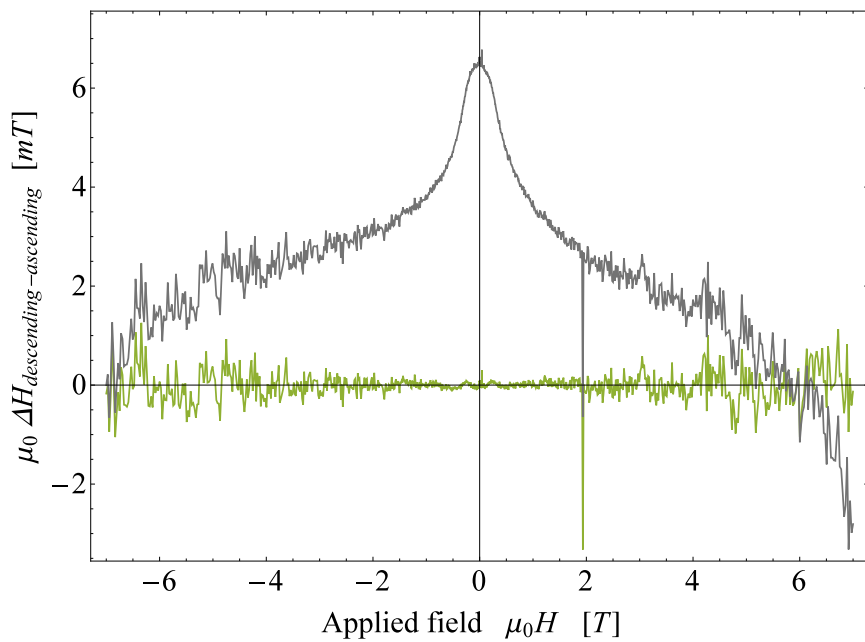


Figure 5: Field difference between descending and ascending branch $\Delta H(H)$ before (grey) and after (green) field correction. Note, that only systematic differences were eliminated, while the random still persist after correction.

Taking into account the whole field range measured, median and median deviation of the absolute values amount to:

- Before correction

$$\tilde{x} = 3.11 \pm 1.28 \text{ mT}, \quad Q_{0.25} = 2.25 \text{ mT}, Q_{0.75} = 4.95 \text{ mT}$$

- After correction

$$\tilde{x} = 0.07 \pm 0.05 \text{ mT}, \quad Q_{0.25} = 0.03 \text{ mT}, Q_{0.75} = 0.18 \text{ mT}$$

Q_{25} and Q_{75} being the 25 and 75% quantiles. The correction proposed reduced the remanent field error by about 98 %.

Next, the method was applied to further $M(H)$ measurements of the Pd standard with lower field ranges. The field error was eliminated in the same efficient manner, *cf.* Fig. 6, albeit for some measurements a 4th order polynomial was used in equations (1) and (2). The parameter vectors are somewhat different, but in general the fitted curve remains similar.

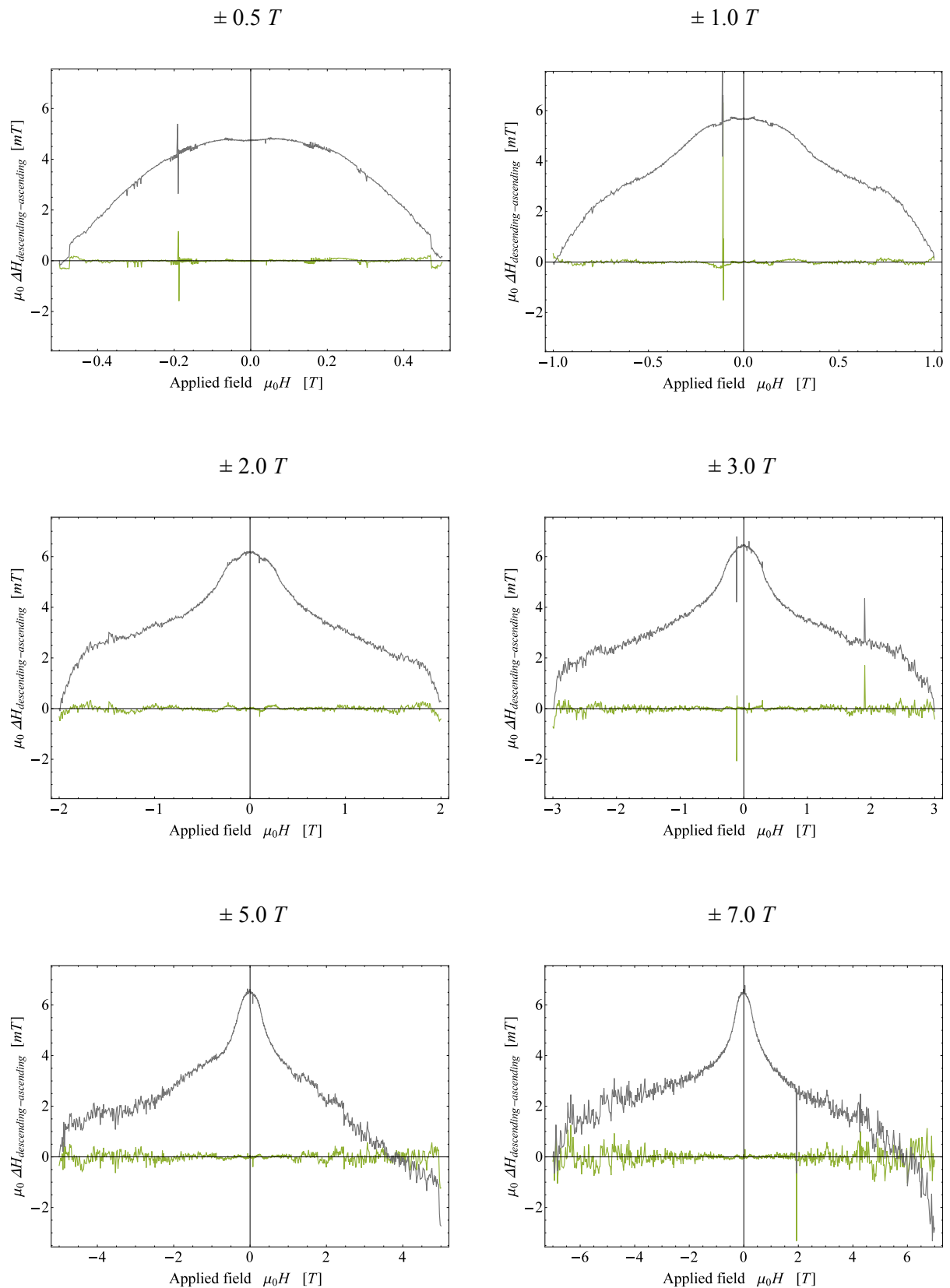


Figure 6: Field difference between descending and ascending branch $\Delta H(H)$ before (grey) and after (green) field correction for $M(H)$ measurements with different field maximal fields. In all cases, the systematic trend resulting from the field error was sufficiently eliminated.

Having a closer look to $M_{corr}(H)$, discontinuities appear in the region where fitting functions changes from $f_P(H)$ to $f_N(H)$ in the descending branch and from $f_N(H)$ to $f_P(H)$ in the ascending branch, cf. Fig. 7. As however the measured hysteresis loops were measured with sufficient resolution this effect is of little importance.

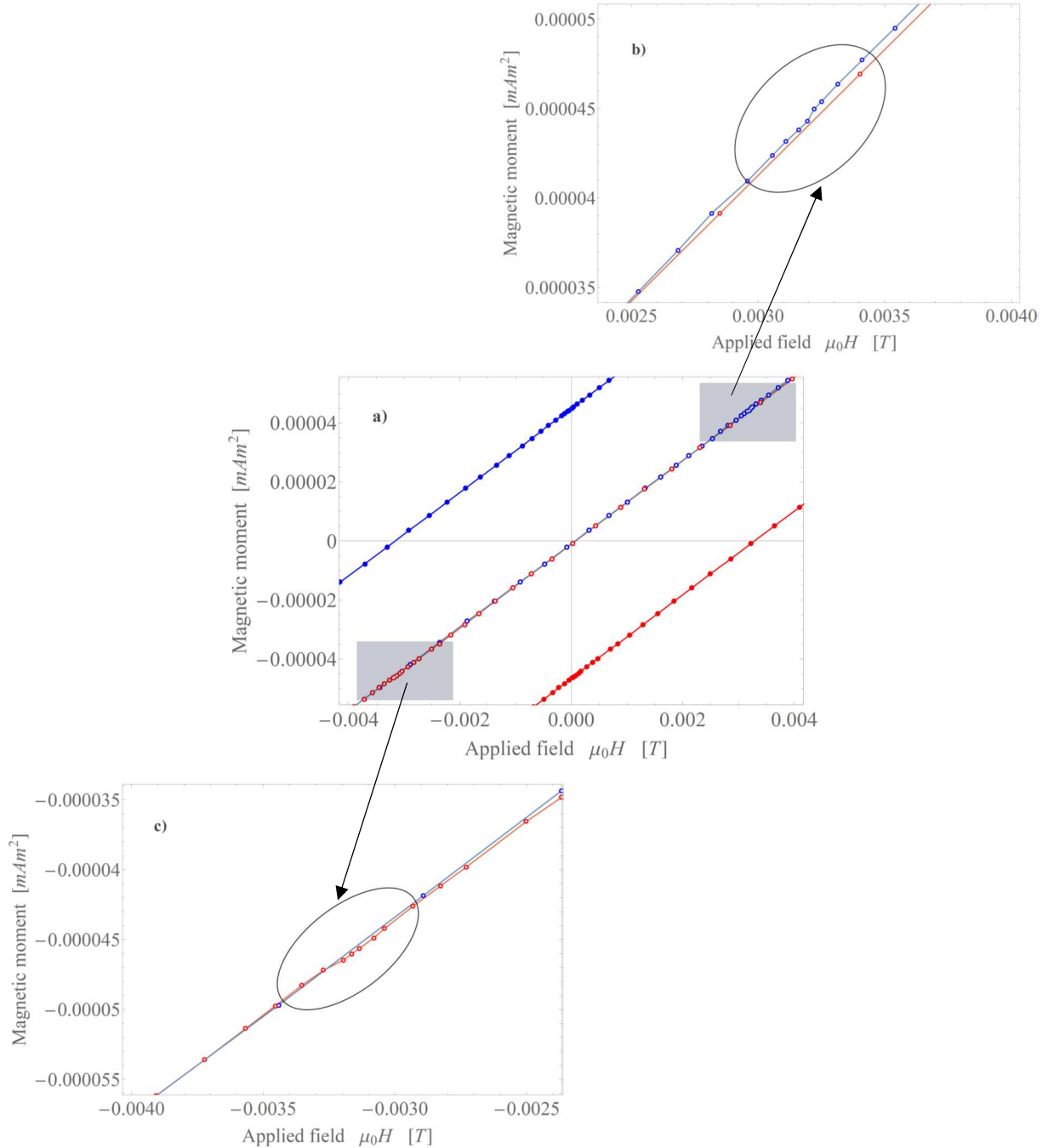


Figure 7: $M(H)$ measurement of the paramagnetic Pd standard sample between ± 3 T. **a)** Zoom of the low field region showing descending (red) and ascending (blue) branches before (filled circles) and after (open circles) remanent field correction. **b) / c)** Further zooms reveal discontinuities in the corrected $M(H)$ curve induced by changing correction functions which are slightly different for $H \rightarrow 0$ and not defined at $H = 0$, cf. text and equations (1), (2).

4. Example of corrected measurements

Magnetic property measurements of dried magnetic nanoparticles are now discussed. Field cooled (FC) hysteresis curves were acquired at 5 and 200 K within a field range of $\pm 3T$. The field during cooling was set to $3T$. In addition, the temperature dependence of the induced magnetisation was investigated by of zero-field cooling (ZFC) and field cooling curves, measured at $5 mT$.

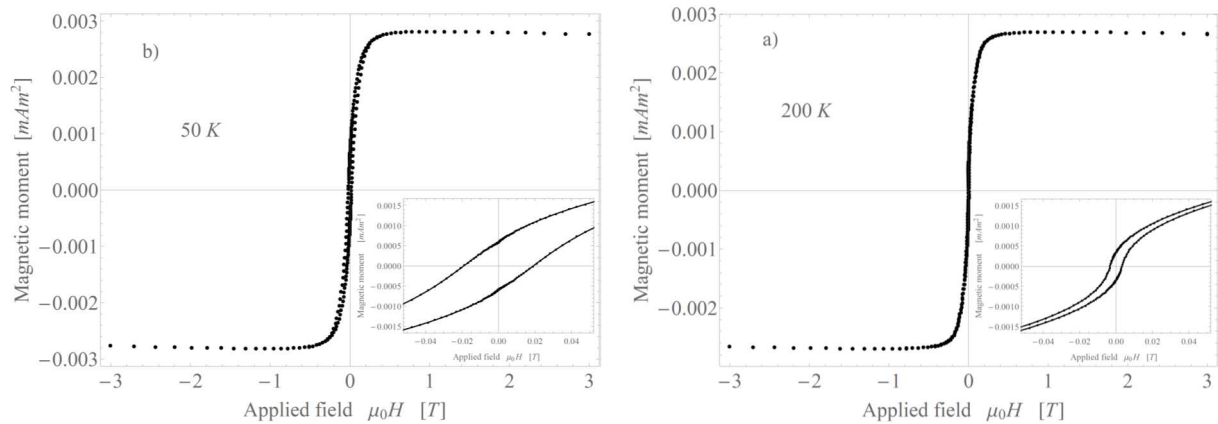


Figure 8: FC cooled hysteresis loops of a magnetic nanoparticle sample measured at 50 and 200 K. The insets are a zoom into the low-field region around 0 T. The field applied during cooling was set to 3 T.

The raw hysteresis data in Figure 8 show that the sample has as single domain behaviour at 50 K and apparently also at 200 K, with the difference that coercive force and saturation remanence at somewhat lower at 200 K, *cf.* insets in Fig. 8a/b. The ZFC/FC warming and cooling curve indicate in contrast that the sample should also be in superparamagnetic state at 200 K and that most of the magnetic moments are blocked around 144 K (Fig. 9a/b), thus well below 200 K. The ZFC/FC curves contradict apparently the hysteresis measurements. The latter indicating still a substantial contribution of blocked moments to the samples’ bulk magnetic moment (*cf.* Fig. 8b).

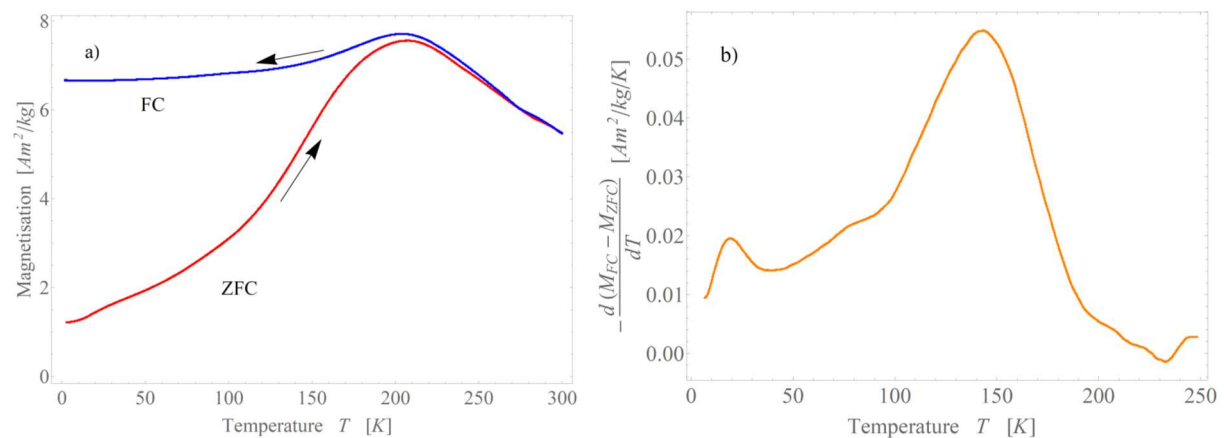


Figure 9: **a)** Continuous zero field cooling / field cooling experiment (ZFC/FC) consisting of about 1800 points each: red –warming curve after ZFC acquired in a field of 5 mT, blue FC curve acquired in the same field. **b)** Blocking temperature distribution calculated from the curves in a) according to recommendations of [4]. A moving average filter with a length of 61 points was applied to ZFC/FC data and to the distribution.

Having in mind the aforementioned remanent field error, the suspicion of erroneous hysteresis measurements is being confirmed when plotting descending and ascending hysteresis branch separately with different colours: Both branches are apparently inverted, and the 200 K measurement is strongly affected by the remanent field error (Fig. 10b).

For field correction, functions $f_P(H)$ and $f_N(H)$ were determined from the corresponding data shown in Figure 6 for $\pm 3T$.

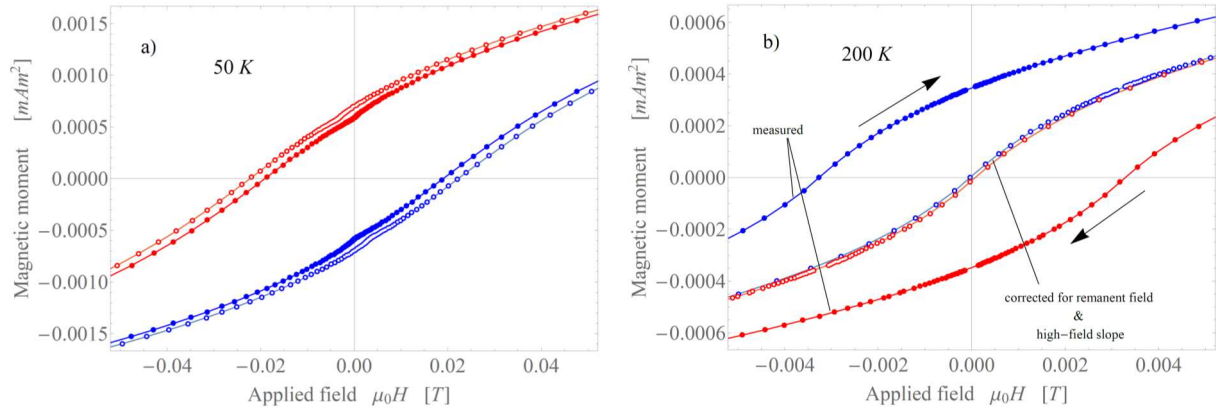


Figure 10: Magnetic hysteresis curves before and after correction. **a)** at 50 K and **b)** at 200 K; zoom into the low field region. Filled circles raw data, open circles data corrected for the remanent field and for high-field slope contributions, latter following the method of approach to saturation [5, 6].

After remanent field correction, the $M(H)$ curves at 200 K cross the field axis at $M \approx 0$. The derived coercive force after remanent field correction and after the not shown high-field slope correction amounts only to 0.056 ± 0.000 mT. Saturation magnetic moment (m_s) and saturation remanent moment (m_{rs}) are 2.77 ± 0.01 mAm² and 8.86 ± 4.46 μ Am² respectively; the ratio m_{rs}/m_s being 0.003. The measurements at 200 K reflect now superparamagnetic behaviour as expected from the ZFC/FC experiments. The remanent field error at 50 K is much less pronounced. Here most of the moments are blocked (stable single domain state) and the sample has a coercive force much higher than the remanent field error.

5. Checks on a different instrument

It may be assumed that the remanent field varies from instrument to instrument, because of the different magnet characteristics. In the following, the correction procedure was applied to measurements from another instrument of exactly the same type. The Pd standard sample was also another. The measurement parameters, cf. chapter 2, were kept unchanged. Figure 11a/b shows that $\Delta H(H)$ looks somewhat different compared to Figures 2/3. Again there is a global maximum peaking at about 6 mT near $H = 0$ but at stronger fields there are significant differences. Consequently equations (1) and (2) were adopted to represent $\Delta H(H)$ as best as possible. While the $Tanh$ term in (1) and (2) was kept, the 5th order polynomial was replaced by one of 11th order for appropriate fitting, cf. Fig. 11a.

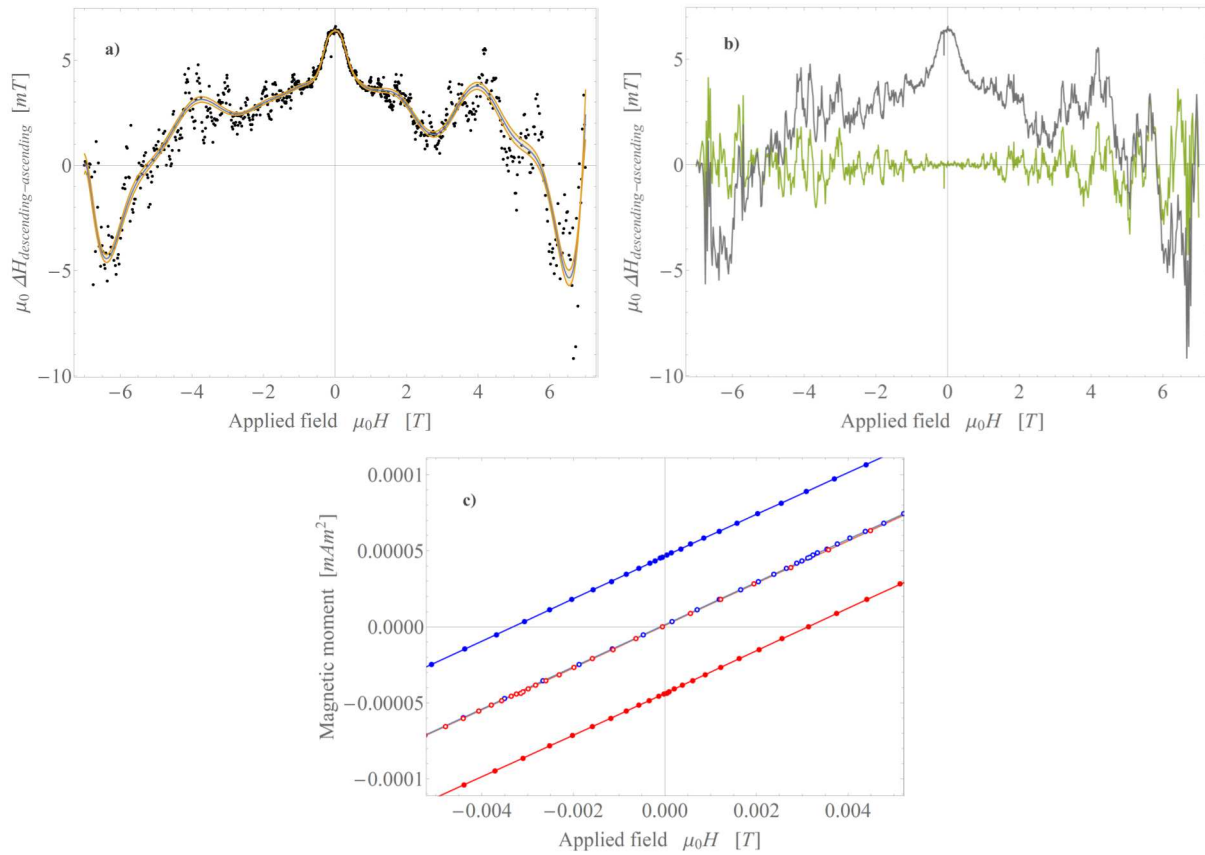


Figure 11: Plots as in Figs. 3, 4 and 5, but for measurements of another Pd standard sample on another instrument of the same type.

For the whole field range, median and median deviation amount to:

- Before correction

$$\tilde{x} = 3.61 \pm 1.26 \text{ mT}, \quad Q_{0.25} = 2.34 \text{ mT}, Q_{0.75} = 4.79 \text{ mT}$$
- After correction

$$\tilde{x} = 0.2 \pm 0.18 \text{ mT}, \quad Q_{0.25} = 0.05 \text{ mT}, Q_{0.75} = 0.61 \text{ mT}$$

Again, the correction successfully reduced the contribution of the remanent field up to 94 %. The test on the second instrument confirms the supposition, that the magnet characteristics vary between instruments and in turn generate slightly different $\Delta H(H)$ curves. Consequently it is indicated to determine for each instrument own correction functions $f_P(H)$ and $f_N(H)$.

6. Final considerations

The method proposed in this technical note removes efficiently the field error caused by the remanent field of the superconducting magnet in magnetic property systems without field feedback compensation.

- The remanent field of the superconducting magnet is temperature independent and reproducible. When comparing different instruments the median of $\Delta H(H)$ before corrections is very similar.
- In contrast, the trend of $\Delta H(H)$ varies from instrument to instrument and is not linear. Therefore, the functions to be established for suppressing this trend are not universally

applicable. It is strongly recommended to establish for each instrument a separate function and to repeat these measurement from time to time.

- The trend of $\Delta H(H)$ may be asymmetric when comparing positive and negative field. It was not tested if this asymmetry inverses when starting the $M(H)$ measurement in the 3rd Quadrant, e.g. $-7 T \rightarrow 0T \rightarrow +7T \rightarrow 0T \rightarrow -7T$.
- This correction is particularly essential for materials with low or zero coercive forces, e.g. dia- para-, superparamagnetic and magnetically viscous materials. Others with higher coercive forces are less affected.
- A shortfall of the method proposed are small possible discontinuities and therefore it is recommended to measure at high resolution when determining the field correction.

7. Acknowledgements

Daniel Ortega from IMDEA Nanociencia (Madrid, Spain) is thanked for providing the magnetic nanoparticle test sample and the enterprise LOT-QD in Darmstadt for providing test measurement data. This technical note is based upon work from COST Action RADIOMAG (TD1402), supported by COST (European Cooperation in Science and Technology).

8. References

- [1] Quantum Design 2016. Magnetic Property Measurement System®, MPMS 3 User's Manual, Part Number 1500-100, F1, 15th edition.
- [2] McElfresh, M, Li, S. & R. Sager 2003, 2016. Effects of Magnetic Field Uniformity on the Measurement of Superconducting Samples. *Quantum Design Application Note*, 1–37.
- [3] Quantum Design 2010. *Application Note 1500-011*, 1–8.
- [4] Bruvera, I.J., Mendoza Zelis, P., Pilar Calatayud, M., Goya, G.F. & F.H. Sanchez 2015. Determination of the blocking temperature of magnetic nanoparticles: The good, the bad, and the ugly. *Journal of Applied Physics* **118**, 184304.
- [5] Bertotti, G., 1998. *Hysteresis in Magnetism*. Academic Press, San Diego.
- [6] Fabian, K. 2006. Approach to saturation analysis of hysteresis measurements in rock magnetism and evidence for stress dominated magnetic anisotropy in young mid-ocean ridge basalt. *Physics of the Earth and Planetary Interiors* **154**, 299–307.